A THERMO-HYDRO-MECHANICAL MODEL OF A HOT DRY ROCK GEOTHERMAL RESERVOIR

Presentor ： Wu, Zi-You
Adviser：Wang, Shih-Jung
Date ：2023.12.22

Outline

- Introduction
- Methodology
- Results
- Conclusions

What is HDR(hot dry rock)

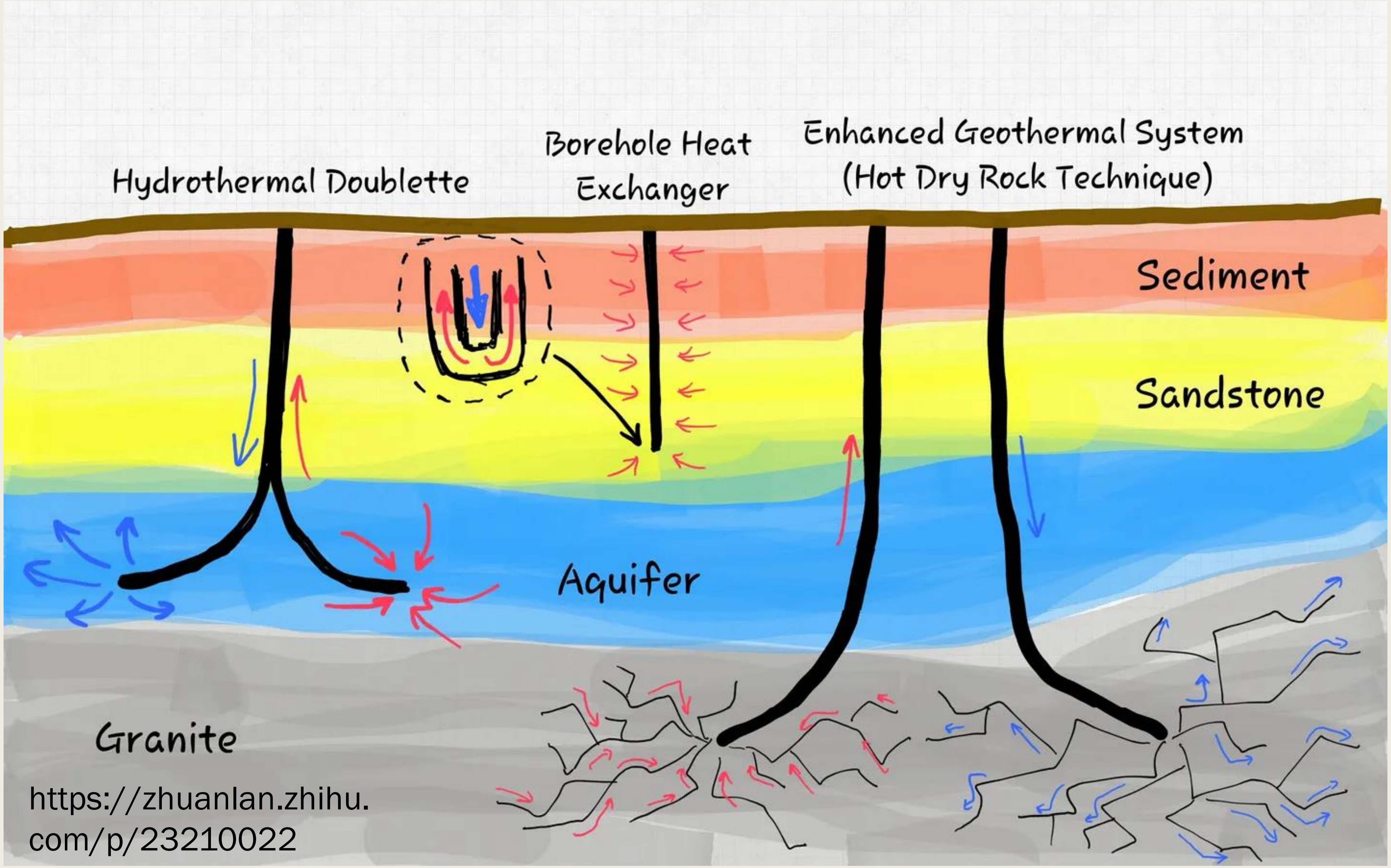

https://zhuanlan.zhihu.com/p/23210022

- HDR geothermal energy reservoir must be:
- (1) engineered ,means created within an impermeable formation of hot crystalline rock
- (2) confined, relates to the state of being enclosed at the boundaries, with negligible water loss.
- (3) created by hydraulic pressurization . refers to the application of enough pressure to reopen sealed/closed joints at depth in a hot crystalline rock mass.
- An HDR geothermal reservoir is a human-made system; therefore, most of its operating parameters can be controlled for optimum productivity, including production temperature, reservoir size, injection conditions of flow rate and pressure, amount of reservoir growth, and placement number of production wellbores

Introduction

- Based on the Thermo-hydro-mechanical (THM) theory, this research establishes a three-dimensional numerical model to conduct development evaluation of hot dry rock (HDR) geothermal reservoirs. This research uses the COMSOL Multiphysics software based on the finite element method(FEM) for simulation and analysis. This paper examines four factors: fracture porosity, fracture permeability, water injection well location, and fracture permeability.
- This paper conducts analysis using a single planar fracture HDR system and multiple planar fracture systems to determine the impact of wellbore arrangement and location on reservoir parameters and productivity.

Methodology

- 1. The porous medium is fully saturated with a single fluid.
- 2. The fluid flow condition obeys Darcy's law.
- 3. Fluid properties change with temperature.
- 4. The heat transfer process obeys Fourier's law with a local thermal balance between the rock matrix and fluid.
- 5. The rock matrix is homogeneous and isotropic.
- 6. The fracture aperture, permeability and stiffness change with pore pressure and effective stress.

1.Mechanical deformation equations

- Force equilibrium equation

$$G\nabla^2 u_i + (\chi + G)u_{j,jj} - \frac{\alpha E}{1-2\upsilon}\nabla T + F = 0 \quad (1)$$

  - *E* is Young's modulus
  - *F* is the body or external force
  - *G* is the shear modulus
  - *u* is the displacement
  - X is the lame constant
  - G is the shear modulus
  - α is the thermal expansion coefficient
  - v is the Poisson's ratio

- Equation is the Expression describing the rock matrix deformation with its corresponding stress distribution.

2. Fracture aperture changes with stress

The coupled effect of the mechanical process on the fluid flow is achieved via the pore pressure, fracture aperture by the changes in the effective stress.

- The parallel plate principle is employed for the representation of the fracture aperture. The effective stress acting on the fracture plane is expressed.
- σ_n is the normal stress acting on the fracture
- σ_n' is the effective stress acting on the fracture
- α_b is the Biot's coefficient
- P is the pore pressure.

$$\sigma_n' = \sigma_n - \alpha_b p \quad (2)$$

- The fracture aperture variation with stress
- b is the fracture aperture
- b0 is the initial aperture
- bmax is the maximum aperture closure
- bres is the residual aperture
- K_n is the normal fracture stiffness

$$b = b_0 - \frac{\sigma_n'}{K_n + \frac{\sigma_n'}{b_{\max}}} + b_{res} \quad (3)$$

- K_n is the fracture normal stiffness
- K_{ni} is the initial fracture normal stiffness
- σ'_n is the effective normal stress acting on the fracture,
- JCS is the joint compressive strength.
- JRC is the joint roughness coefficient.
- $b_{\max}$ is the maximum fracture closure.
- A; B; C and D are constants determined experimentally.
- σ'_n equation ,b and K_n equation is the important equation of fluid flow influences the mechanical process

$$K_n = K_{ni}\left(1 - \frac{\sigma'_n}{K_{ni}b_{\max} + \sigma'_n}\right)^{-2} \quad (4)$$

$$K_{ni} = 0.02\left(\frac{JCS}{a_0}\right) + 2JRC - 10$$

$$b_{\max} = A + B(JRC) + C\left(\frac{JCS}{a_0}\right)^{D}$$

3. Fracture fluid flow equations

- The fluid flow in the discrete fracture can also be described using the continuity equation and Darcy's law
- b, $\emptyset_f$ and v_f are the fracture aperture, porosity and Darcy's field velocity.
- The fracture Darcy's field velocity v*f*
- K_f is the fracture permeability
- S is the fracture spacing.
- Important equation of the coupled effect of the mechanical process on the fluid flow is achieved via the fracture permeability.

$$b\frac{\partial}{\partial t}\left(\phi_f \rho_L\right) + \nabla_T \cdot \left(b\rho_L v_f\right) = bQ_m$$

$$v_f = -\frac{\kappa_f}{\mu}\nabla_T p$$

$$\kappa_f = \frac{b^3}{12S} \tag{5}$$

4.Porous medium heat transport equations

- The generalized equation describing the heat transfer mechanism in the porous medium.
- $\left(pC_p\right)_e$ is the effective densities and heat capacities
- T is the temperature
- $C_{p,L}$ is the fluid heat capacity
- q is the Fourier's conductive heat flux
- Q is the heat source/sink term
- The Fourier's conductive heat flux *q* is given as
- λ_e is the effective thermal conductivities
- <u>The fluid flow's coupled effect on the thermal process is accomplished through Darcy's velocity field term</u>

$$(\rho C_P)_e \frac{\partial T}{\partial t} + \rho_L C_{P,L} v \bullet \nabla T + \nabla \bullet q = Q \tag{6}$$

$$q = -\lambda_e \nabla T$$

$$\lambda_e = \phi \lambda_S + (1 - \phi)\lambda_L$$

- λ_S is the rock matrix thermal conductivity and λ_L is the fluid thermal conductivity.

- (7)The thermal process affects the fluid flow via the density, viscosity and thermal conductivity.
- (8)The coupled effect of temperature on viscosity.

(7)
$$\rho_L(T) = 996.9\left(1 - 3.17 \times 10^{-4}(T - 298.15) - 2.56 \times 10^{-6}(T - 298.15)^2\right)$$

(the temperature ranges between 20^oC and 250^oC)

(8)
$$\mu(T) = 2.414 \times 10^{-5} \times 10^{\frac{247.8}{(T+133)}}$$

(the temperature ranges between 4^oC and 250^oC)

- The coupled effect of the mechanical process on the fluid flow is achieved via the pore pressure, fracture permeability and aperture by the changes in the effective stress.

THM coupled processes framework

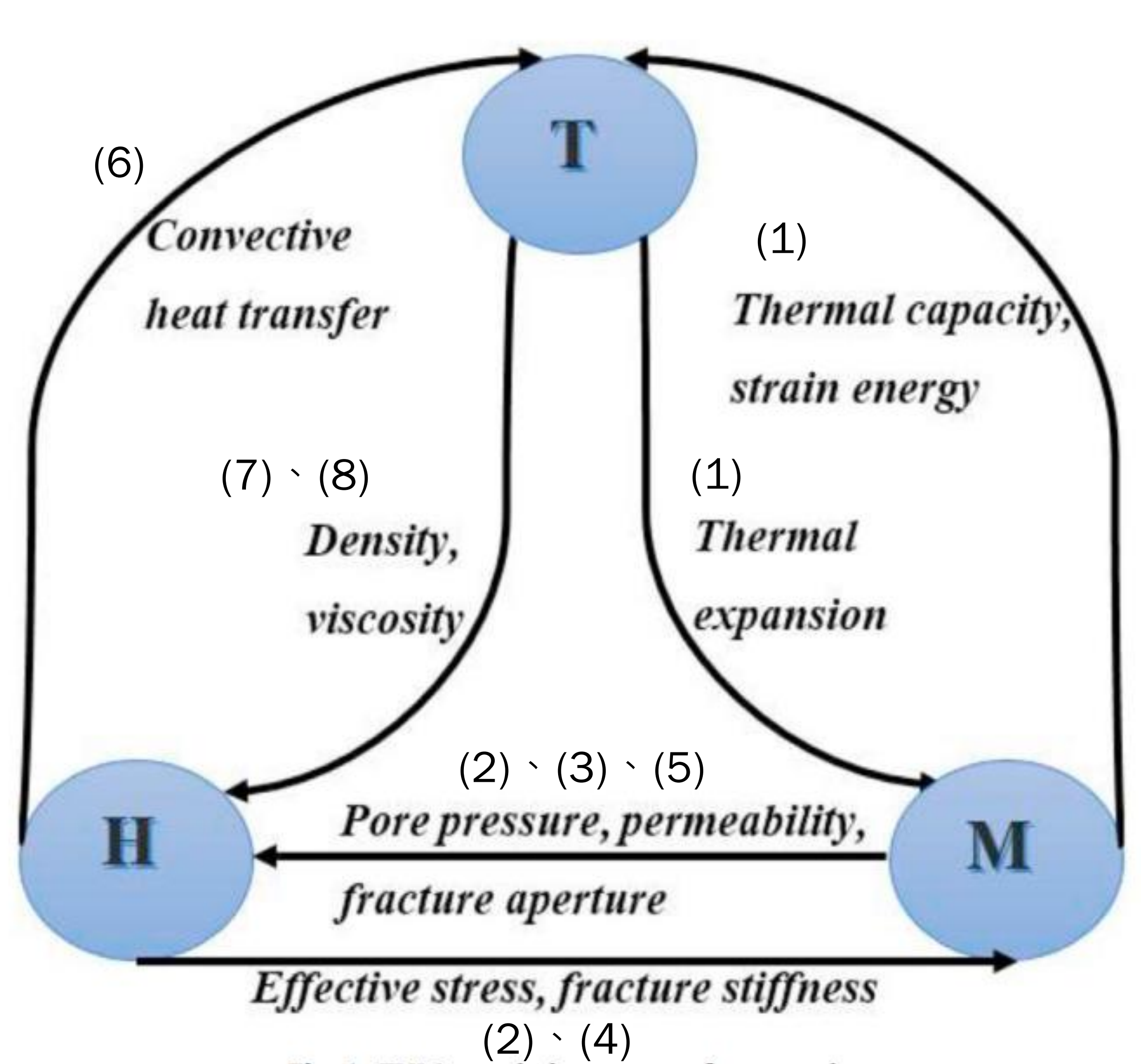

Fig. 1. THM coupled processes framework.

- Results

- (1) comparison of reservoir parameters and productivity between aligned and unaligned wellbore configurations using a <u>single planar HDR system.</u>
- (2) in-depth analysis of several reservoir parameters that determine HDR system performance and productivity, employing the concept of <u>multiple planar fractures and focusing on wellbore placement.</u>

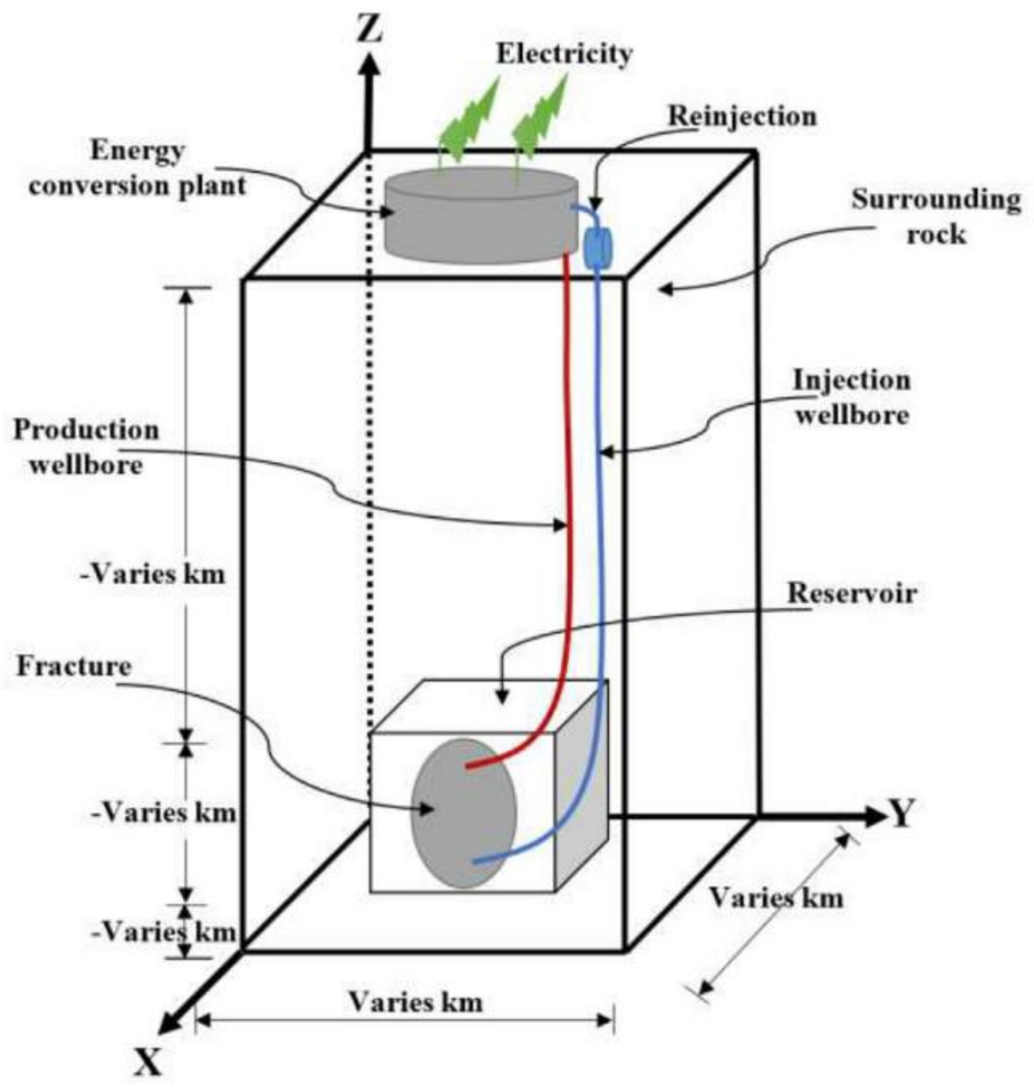

a. Schematic representation of the HDR geothermal reservoir

Fig. 4a. Schematic representation of the HDR geothermal reservoir.

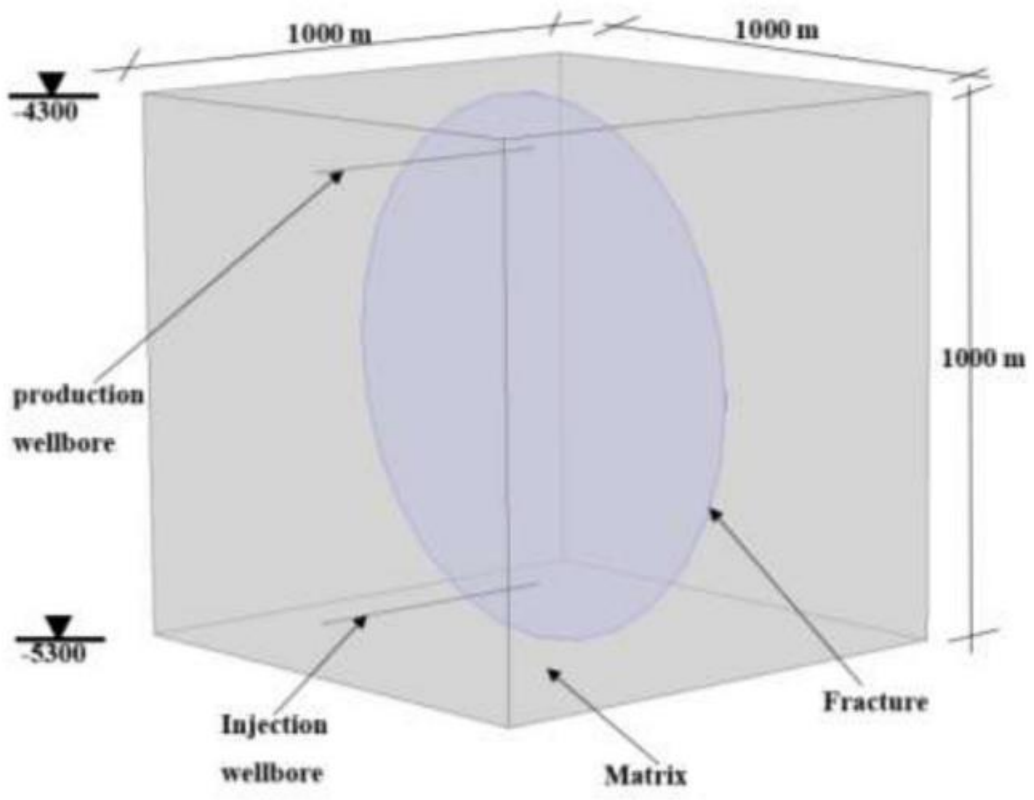

b. Case study one reservoir geometry

Fig. 4b. Case study one reservoir geometry.

- This case study investigates the potential of energy extraction from HDR geothermal reservoirs under six different configurations using a coupled model of THM processes.
- Fig. 5 presents the con figurations of each of the scenarios. In each one, the reservoir properties and the initial and boundary conditions remain the same. The reservoir geometry, including matrix and fracture, is the same for all the scenarios; the only differences relate to the wellbore position.

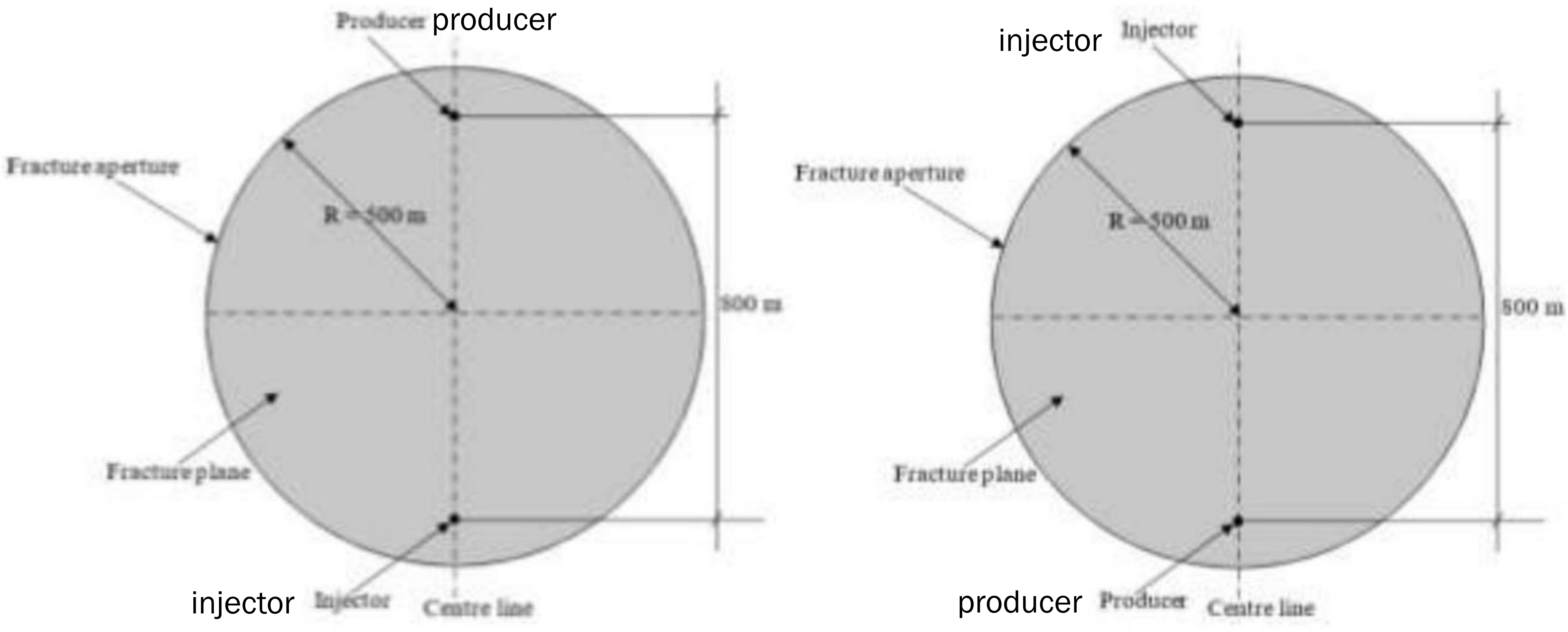

a. Case 1 **b.** Case 2

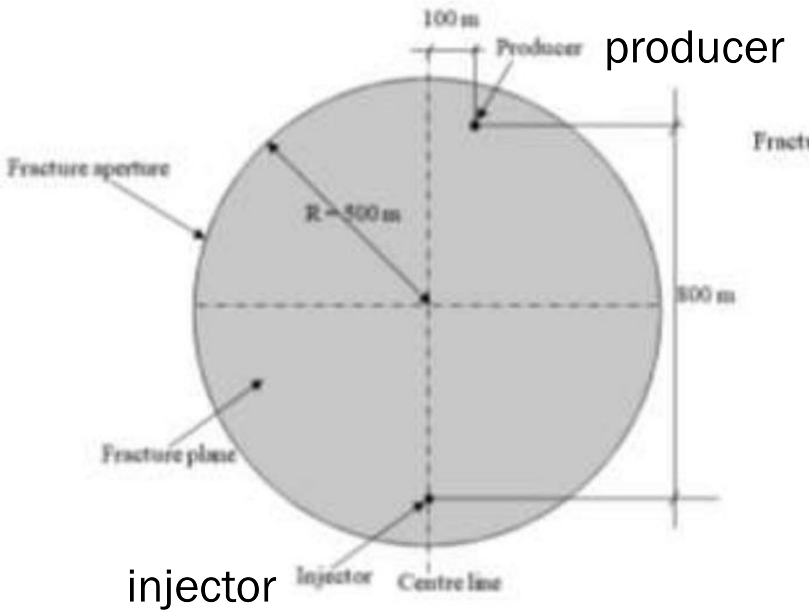

c. Case 3

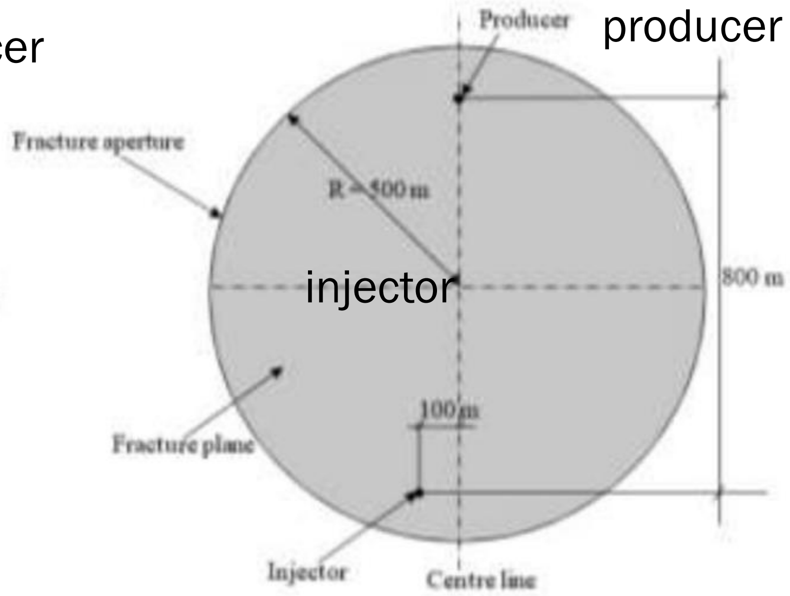

d. Case 4

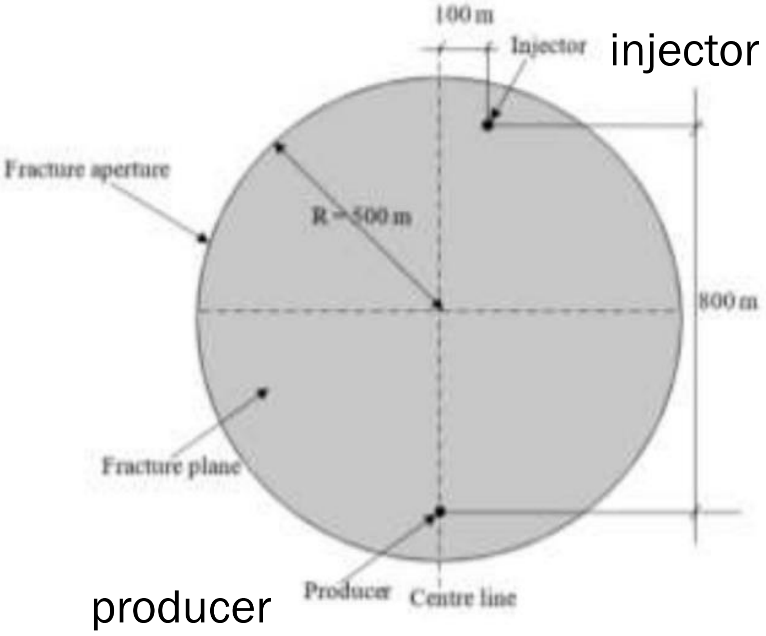

e. Case 5

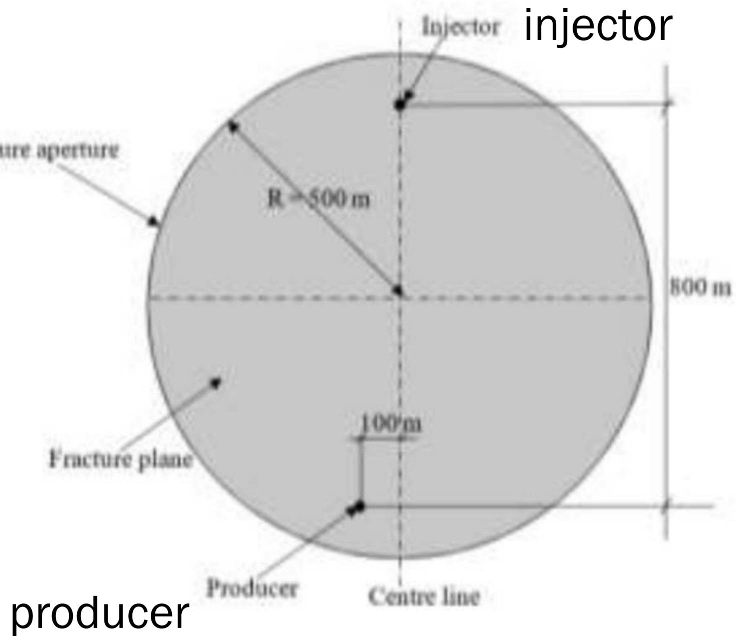

f. Case 6

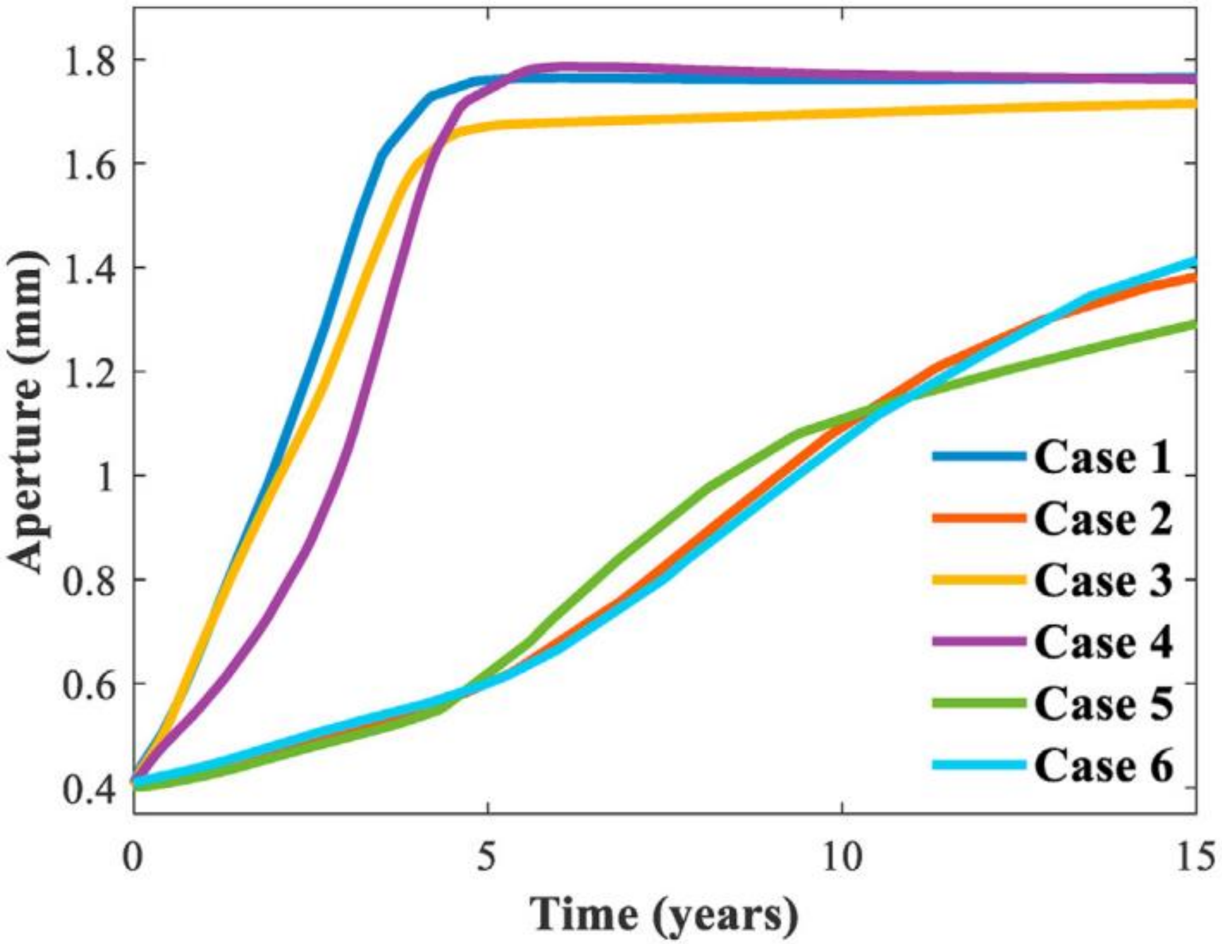

Fig. 6. Fracture aperture changes with time for the six different reservoir configurations.

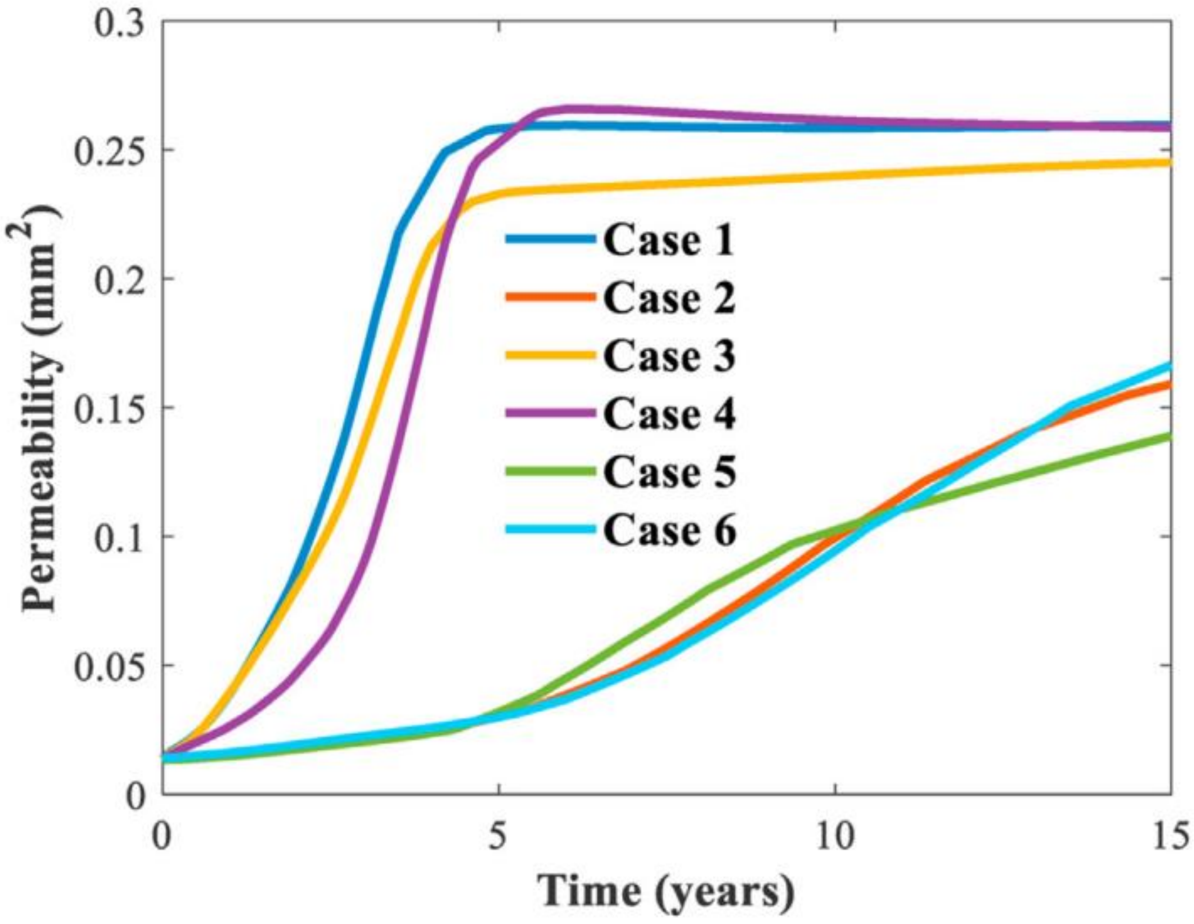

Fig. 7. Fracture permeability changes with time for the six different reservoir configurations.

- injection wellbore in top(case 2 5 6) or in bottom(case 1 3 4)
- possible reason for the behaviour is that cases 1, 3 and 4 tend to have higher stress because of the location of the wellbore at the fracture bottom, so the more significant increase in the fracture aperture during the first few years. in cases 2, 5 and 6, the stress is lower because the wellbore is located at the reservoir top, leading to a smaller and more gradual increase in the aperture.

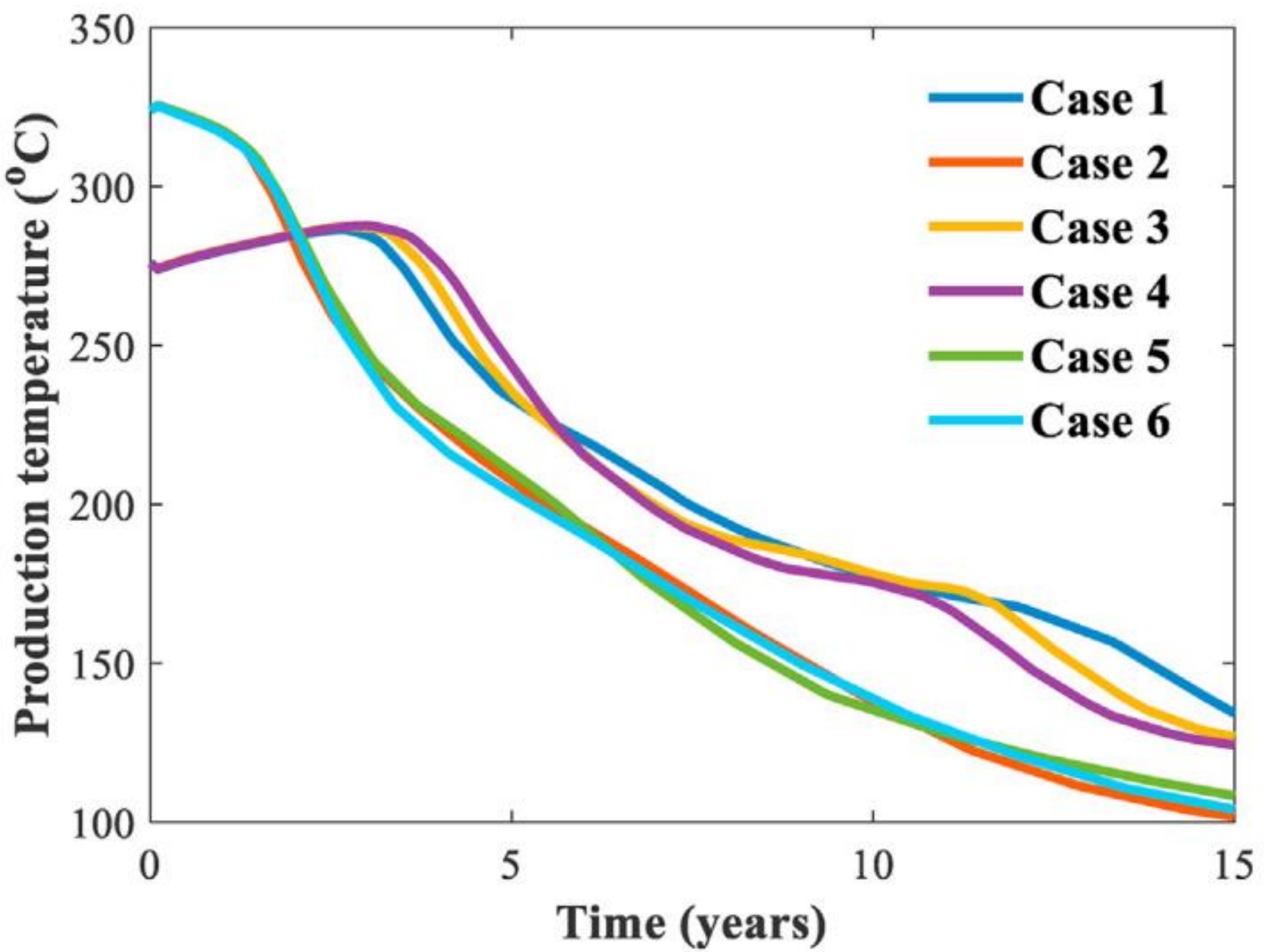

Fig. 8. Production temperature for the six different reservoir configurations.

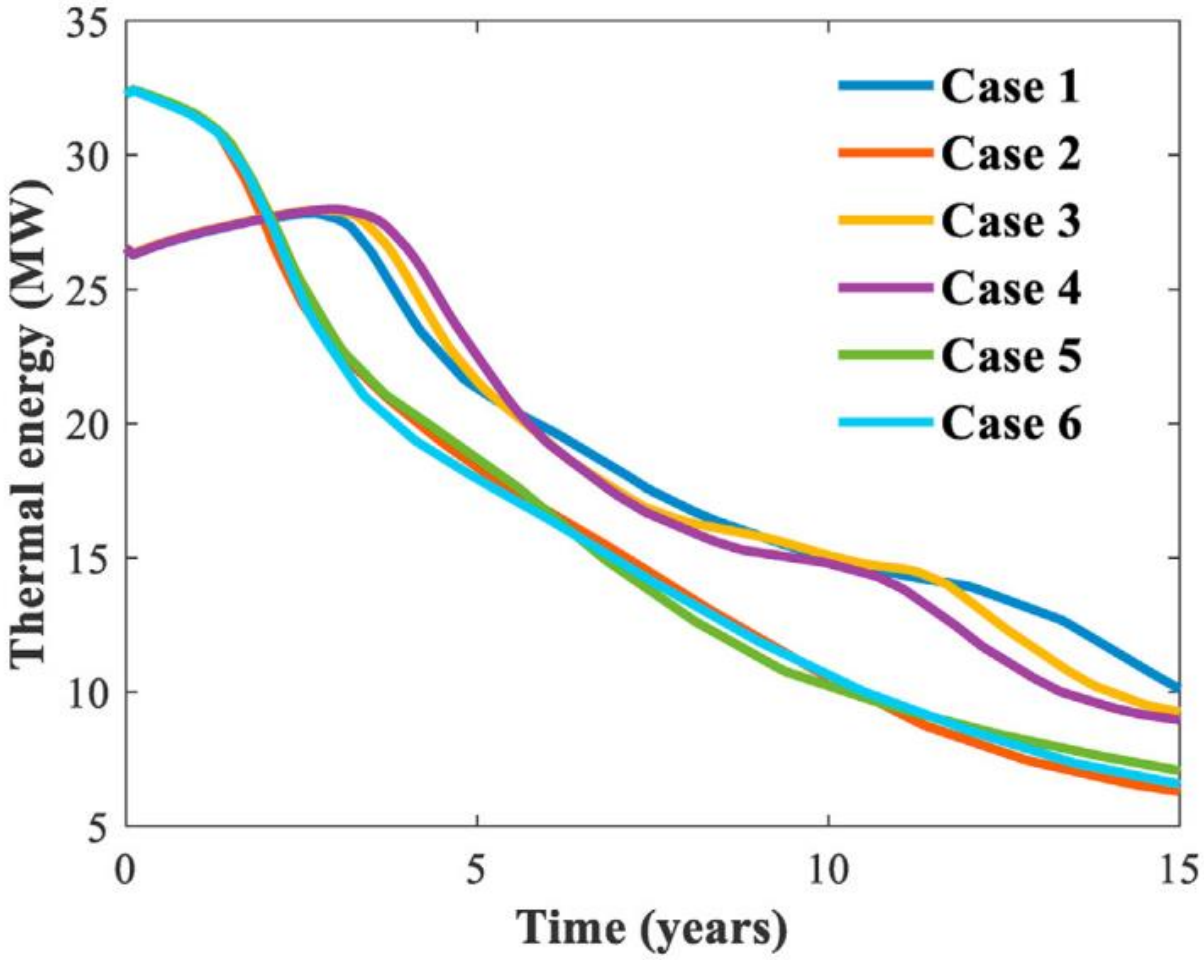

Fig. 9. Thermal energy at the production wellbore for the six different reservoir configurations.

- Fig. 8 and 9 show the production temperature and thermal energy curves at the production wellbore for the different scenarios.
- injection wellbore in top(case 2 5 6) or in bottom(case 1 3 4)

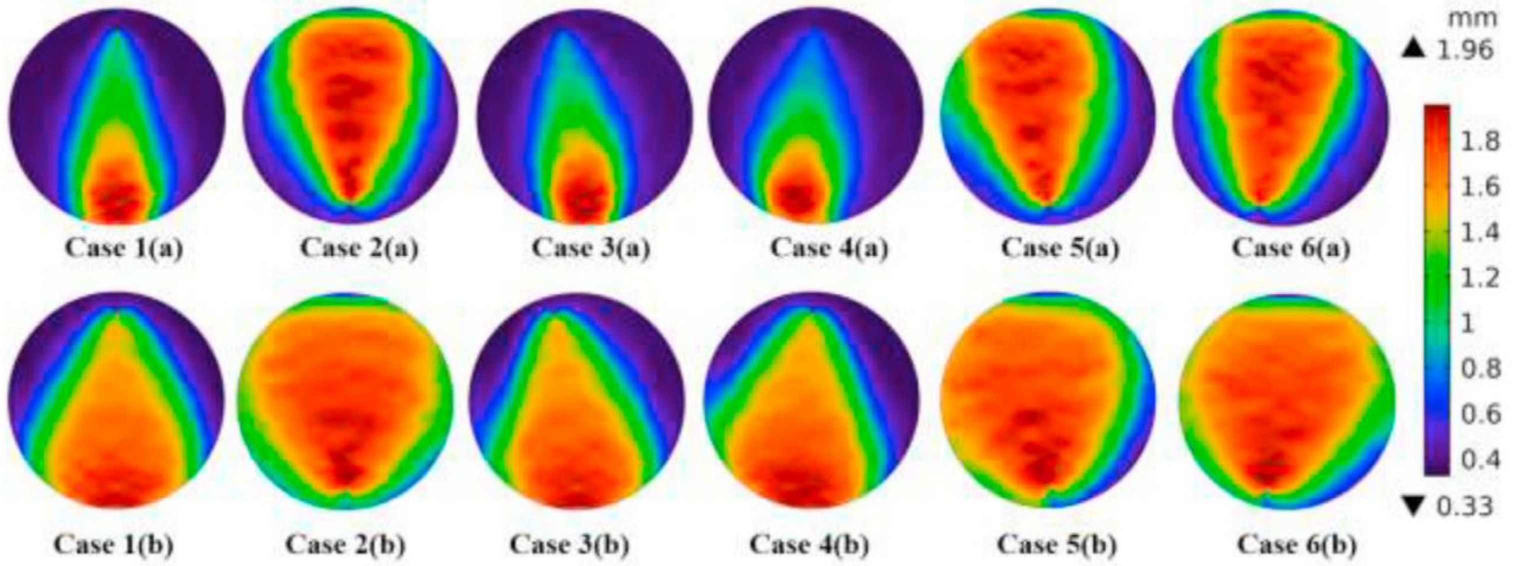

Fig. 10. Aperture changes for the different cases simulated at 5 years (a) and 10 years (b).

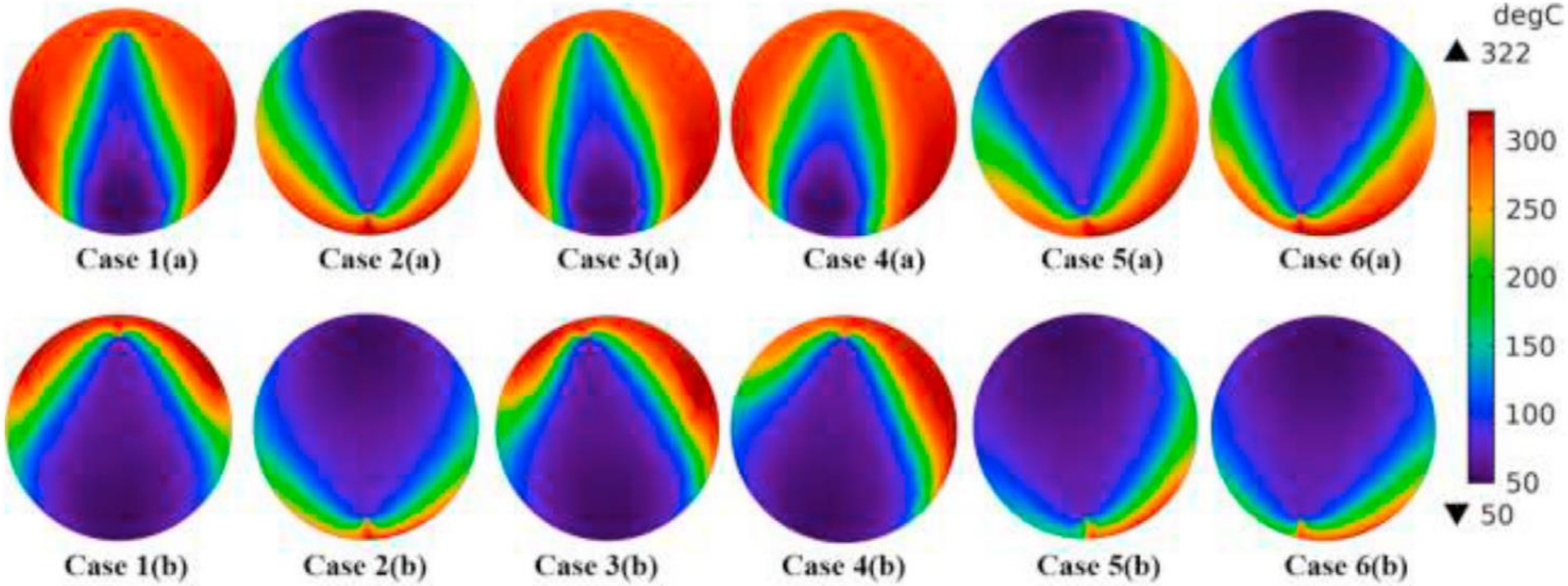

Fig. 12. Thermal front evolution for the different cases simulated at 5 years (a) and 10 years (b).

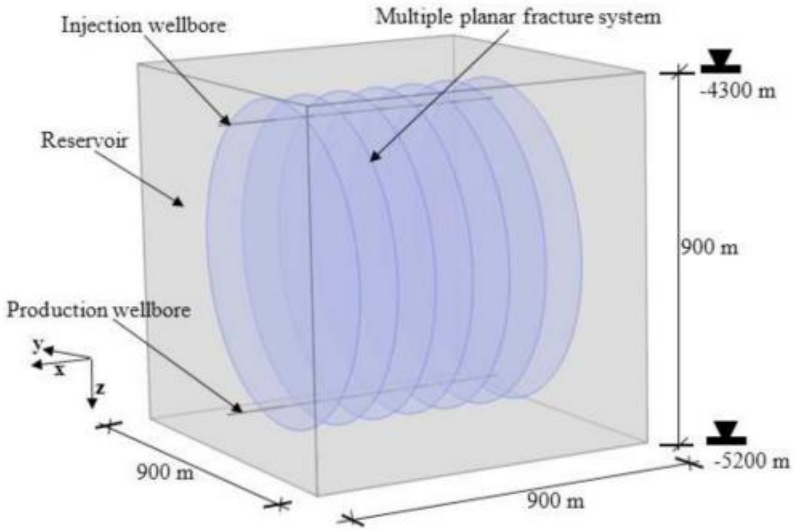

a. Top-bottom (TB) reservoir geometry

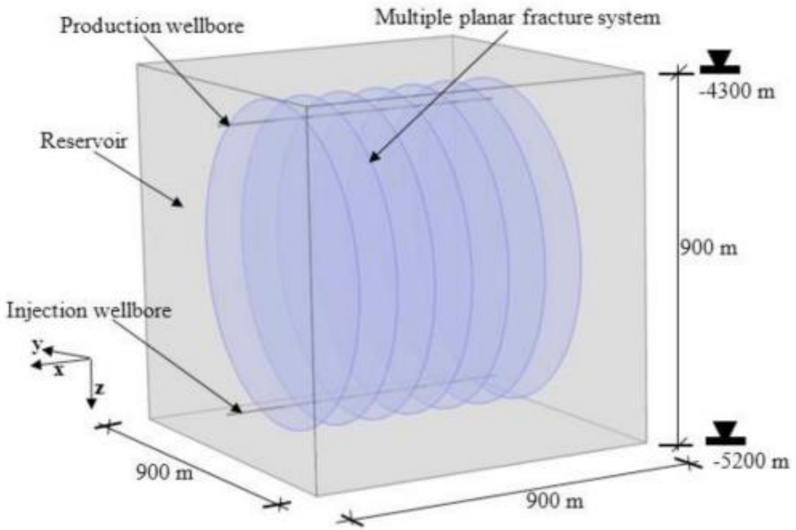

b. Bottom-top (BT) reservoir geometry

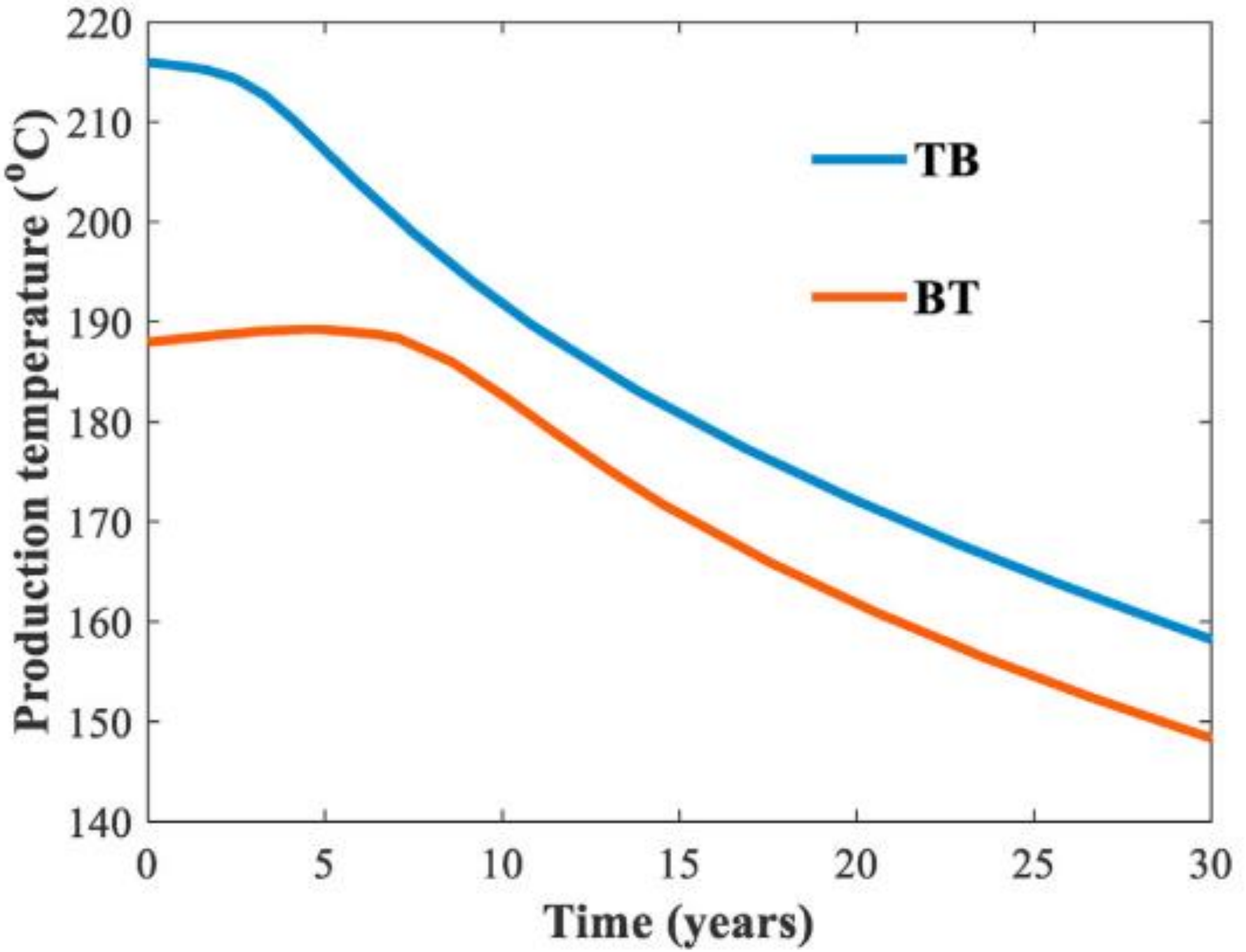

Fig. 14. Production temperature for the top-bottom (TB) and bottom-top (BT) cases.

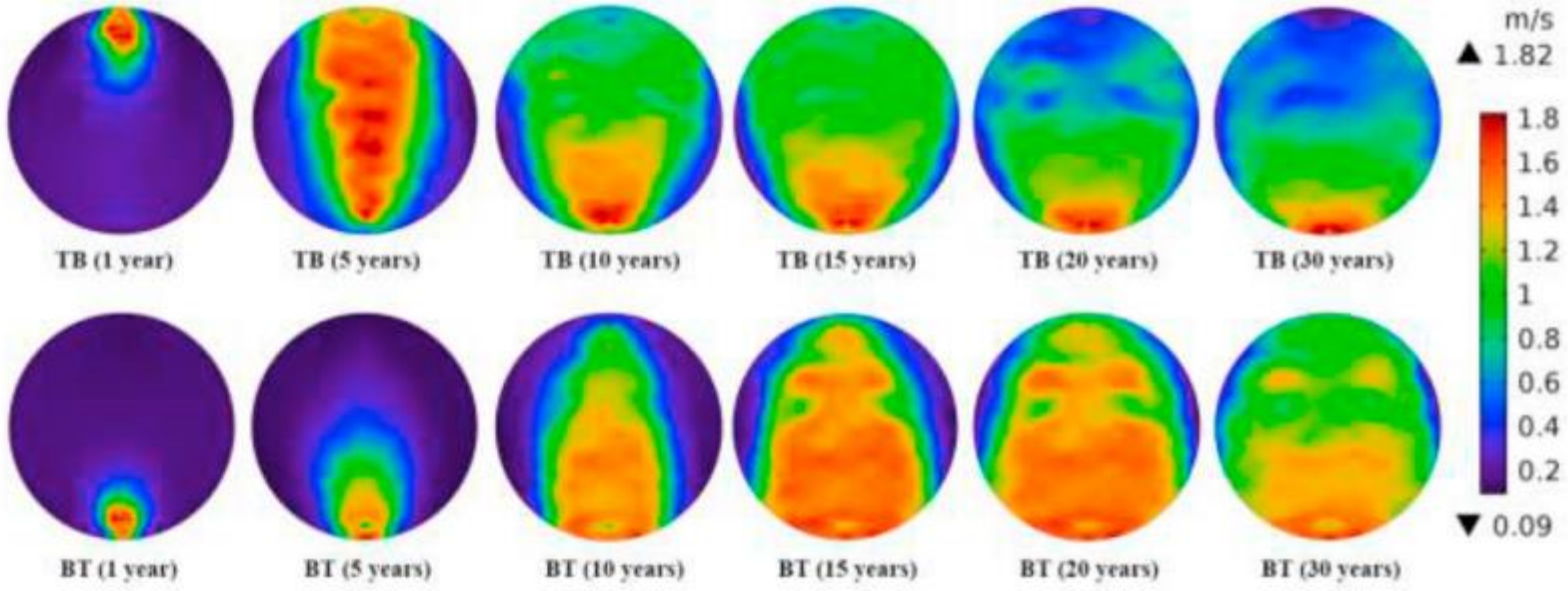

Fig. 21. Fracture conductivity evolution on the middle fracture surface for top-bottom (TB) and bottom-top (BT) scenarios.

- Fracture conductivity is described as the product of fracture permeability and fracture aperture. because it determines the productivity of wellbores after stimulation.
- The bottom-top case creates better conductivity compared to the top-bottom scenario because the fracture aperture opening is more extensive, resulting in high conductivity.

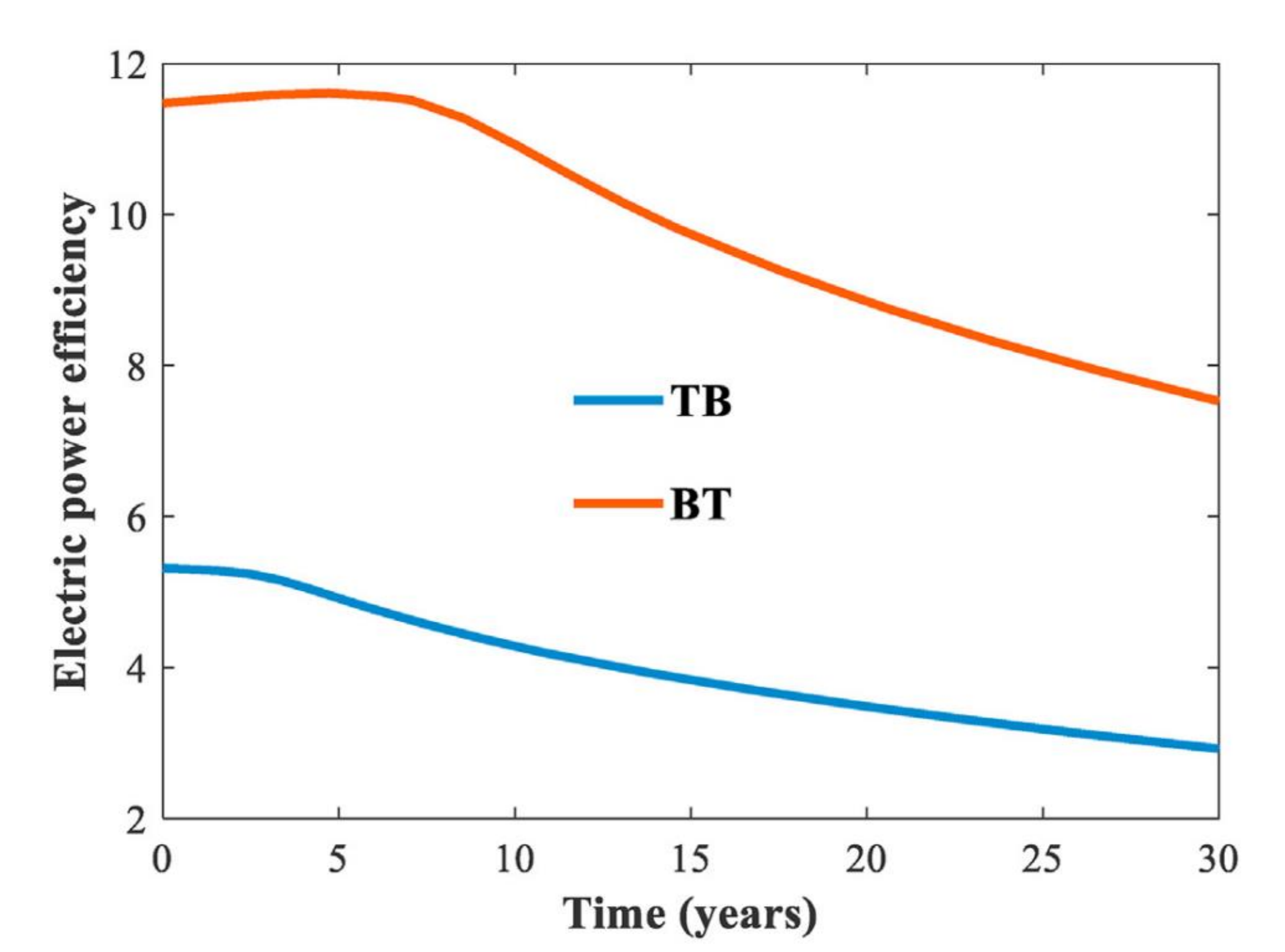

$$\eta_T = \frac{E_T}{EPT} = \frac{\rho_L \eta_P (mC_{P,L}(T - T_{inj}))}{(P_{inj} - P_{pro}) - \rho_L g(z_{inj} - z_{pro})}$$

- Energy efficiency in a geothermal system is calculated as the ratio of total thermal or electric energy produced to the internal energy consumed.

P_L is the fluid density
P pressure
Z wellbore depth.
T temperature
$C_{p,L}$ is the fluid heat capacity
EPT The total internal energy consumed
n_T is the pump efficiency
E_T thermal energy production

Conclusions

- results obtained in this investigation for a single planar fracture, wellbore alignment does not have much impact on fracture aperture, fracture permeability, production temperature or thermal energy. On the other hand, the results do show that wellbore placement has a significant effect on all the reservoir parameters analysed.
- It is evident from the results that the bottom-top scenario gives the most efficient output, with substantial improvement in fracture aperture and transmissibility.
- 1. Injection wellbore placement determines the extent to which the productivity of HDR systems might be improved.
- 2. Fracture aperture enhancement is a crucial parameter in geothermal energy mining.
- 3. Fracture transmissibility is an essential parameter that mea sures the flow pathway accessible in a fractured reservoir system.
- 4. The energy efficiency of HDR geothermal reservoirs primarily depends on the fracture permeability.

Thank you for listening.

- Mechanical deformation in a porous medium is described by theconservation of linear momentum.
- F is the body or external force
- σ_{ij} is the total stresstensor

$$\nabla \sigma_{ij} + F = 0$$

- The expression for the deformed rock matrix
- ε_{ij} is the total strain tensor and u is the displacement

$$\varepsilon_{ij} = \frac{1}{2}\left(u_{i,j} + u_{j,i}\right)$$

- The expression for the deformed rock matrix
- X is the lame constant
- G is the shear modulus
- E is Young’s modulus
- α is the thermal expansion coefficient
- E is Young’s modulus
- dij is the Kronecker delta.

$$\sigma_{ij} = 2G\varepsilon_{ij} + \chi\varepsilon_{kk}\delta_{ij} - \frac{\alpha E \Delta T}{1 - 2\upsilon}\delta_{ij}$$

3. Porous medium fluid flow equations

- The continuity equations and Darcy's lawdefine the flow of fluid in the porous medium

$$\frac{\partial}{\partial t}(\rho_L \phi) + \nabla \cdot (\rho_L v) = Q_m$$

- P_L is the fluid density
- Ø is the rock matrix porosity
- v is Darcy's field velocity,
- Qm is the mass source

- k is the rock permeability
- μ is the fluid viscosity

$$v = -\frac{\kappa}{\mu}\nabla p$$

6.Fracture heat transport equations

- Heat transport in the discrete fracture
- n is a vector normal to the boundary
- Q_f is the energy source/ sink term of the fracture,
- p_f is the fracture density,
- $C_{P,L}$ is the fracture heat capacity
- qf is the fracture heat flux.
- The fracture effective densities and conductivities $\left(p_L C_{P,L}\right)_e$

$$-\mathbf{n} \cdot q = bQ_f - b\left(\rho_f C_{P,f}\right)_e \frac{\partial T}{\partial t} - b\rho_L C_{P,L} \upsilon \cdot \nabla_T T - \nabla_T \cdot q_f$$

$$\left(\rho_f C_{P,f}\right)_e = \left(1 - \phi_f\right)\rho_L C_{P,L} + \phi_f \rho_S C_{P,S}$$

$$q_f = -b\lambda_{ef} \nabla T$$

- λ_{ef} is the effective fracture thermal conductivities
- λ_f is the fracture thermal conductivity

Table 1
Material properties of the case study one reservoir.

Parameter	Symbol	Value	Unit
Matrix			
Thermal conductivity	λ_S	3.0	W/m/K
Coefficient of thermal expansion	β_S	7e-6	1/K
Heat capacity	$C_{P,S}$	900	J/kg/K
Rock density	ρ_S	2700	kg/m^3
Young's modulus	E	60	GPa
Poison's ratio	ν	0.25	
Porosity	ϕ	0.2	–
Permeability	κ	1e-18	m^2
Vertical stress	σ_V	67	MPa
Maximum horizontal stress	σ_H	57	MPa
Minimum horizontal stress	σ_h	46	MPa
Biot coefficient	α_b	0.79	–
Biot modulus	M	1.23e4	MPa
Solid bulk modulus	K_S	50	GPa
Fracture			
Thermal conductivity	λ_f	2.5	W/m/K
Heat capacity	$C_{P,f}$	900	J/kg/K
Fracture density	ρ_f	2500	kg/m^3
Young's modulus	E_f	50	GPa
Porosity	ϕ_f	0.1	–
Initial aperture	b_0	0.416	mm
Maximum fracture closure	b_{max}	0.02	mm
Initial fracture stiffness	K_{ni}	1e5	MPa/m

Table 2
Reservoir properties of the multiple planar fracture HDR systems.

Parameter	Symbo	Value
Matrix		
Thermal conductivity	λ_S	3.0
Coefficient of thermal expansion	β_S	7e-6
Heat capacity	$C_{P,S}$	900
Rock density	ρ_S	2700
Young's modulus	E	60
Poison's ratio	ν	0.25
Porosity	ϕ	0.1
Permeability	κ	1e-18
Vertical stress	σ_V	90
Maximum horizontal stress	σ_H	80
Minimum horizontal stress	σ_h	60
Biot coefficient	α_b	0.79
Biot modulus	M	1.23e4
Solid bulk modulus	K_S	50
Fractures		
Thermal conductivity	λ_f	2.5
Heat capacity	$C_{P,f}$	900
Fracture density	ρ_f	2500
Young's modulus	E_f	50
Porosity	ϕ_f	0.01
Initial aperture	b_0	0.221
Maximum fracture closure	b_{max}	0.02
Initial fracture stiffness	K_{ni}	1e5

Validation study

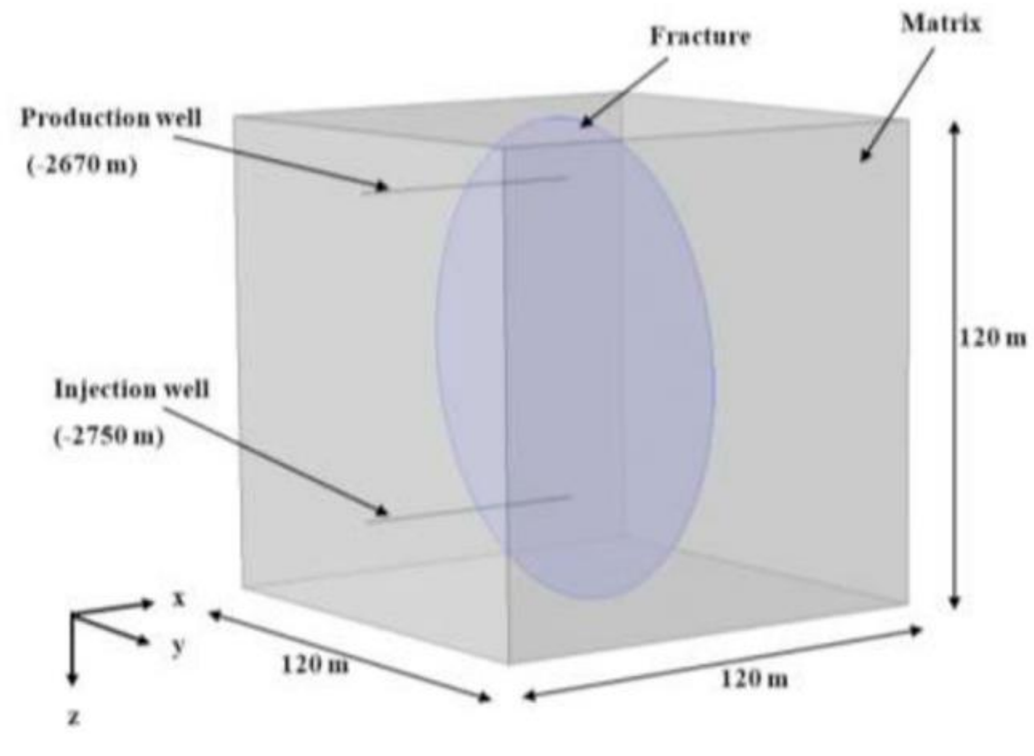

Fig. 2. Representation of the Fenton Hill Phase I HDR system.

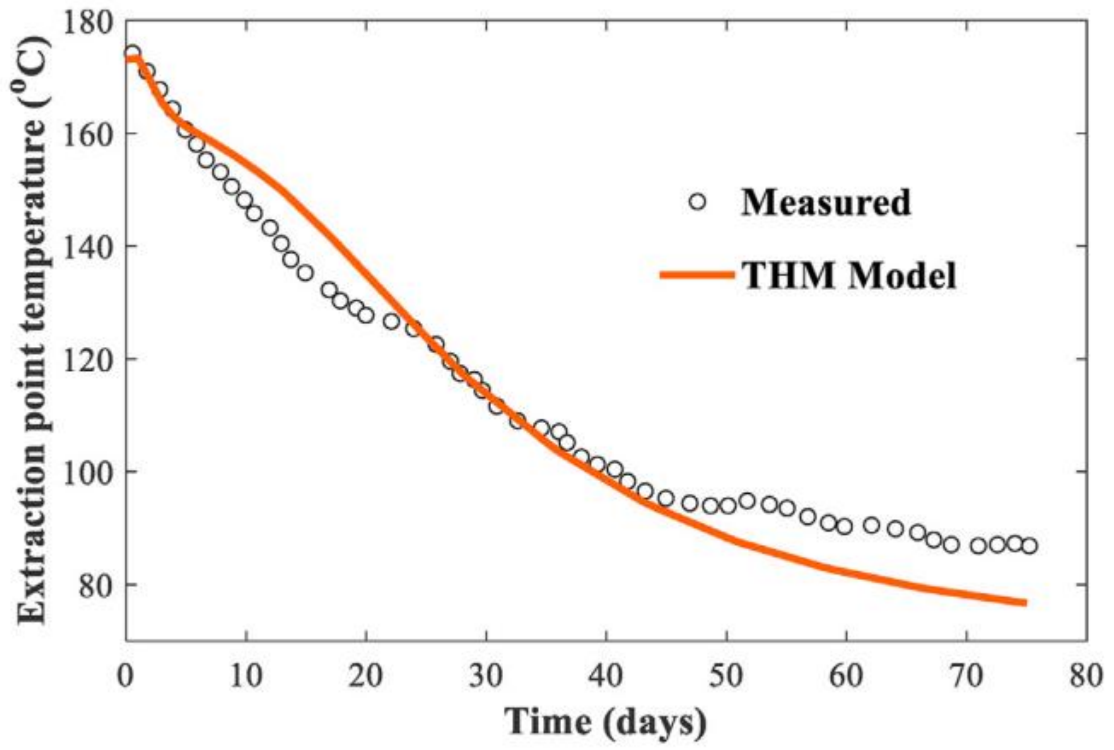

Fig. 3. Simulation and measured results for extraction point temperature vs. time.

- Similarly, the fluid flow influences the mechanical process through effective stress and fracture stiffness by variations in the pore pressure.
- the temperature affects fluid density changes over time.
- using the thermal expansion coefficient for the thermal process in addition to the thermal capacity and strain energy for the mechanical process.

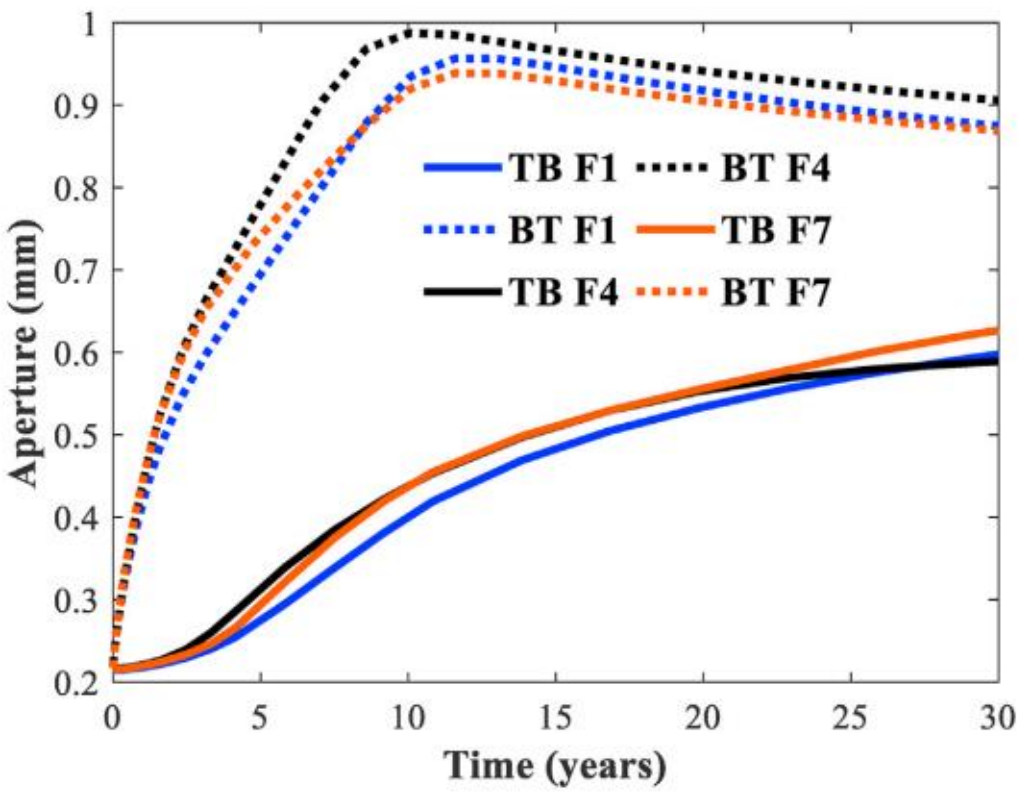

Fig. 24. Fracture aperture changes for the top-bottom (TB) and bottom-top (BT) cases.

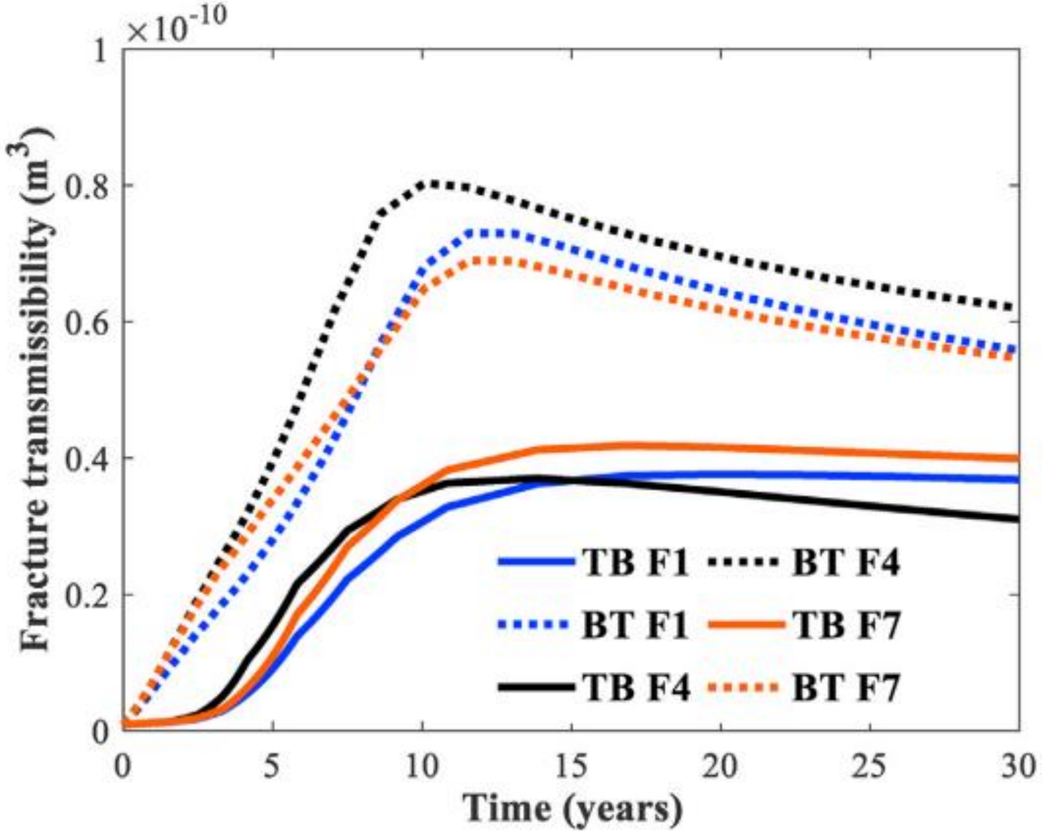

Fig. 25. Fracture transmissibility for the top-bottom (TB) and bottom-top (BT) cases.

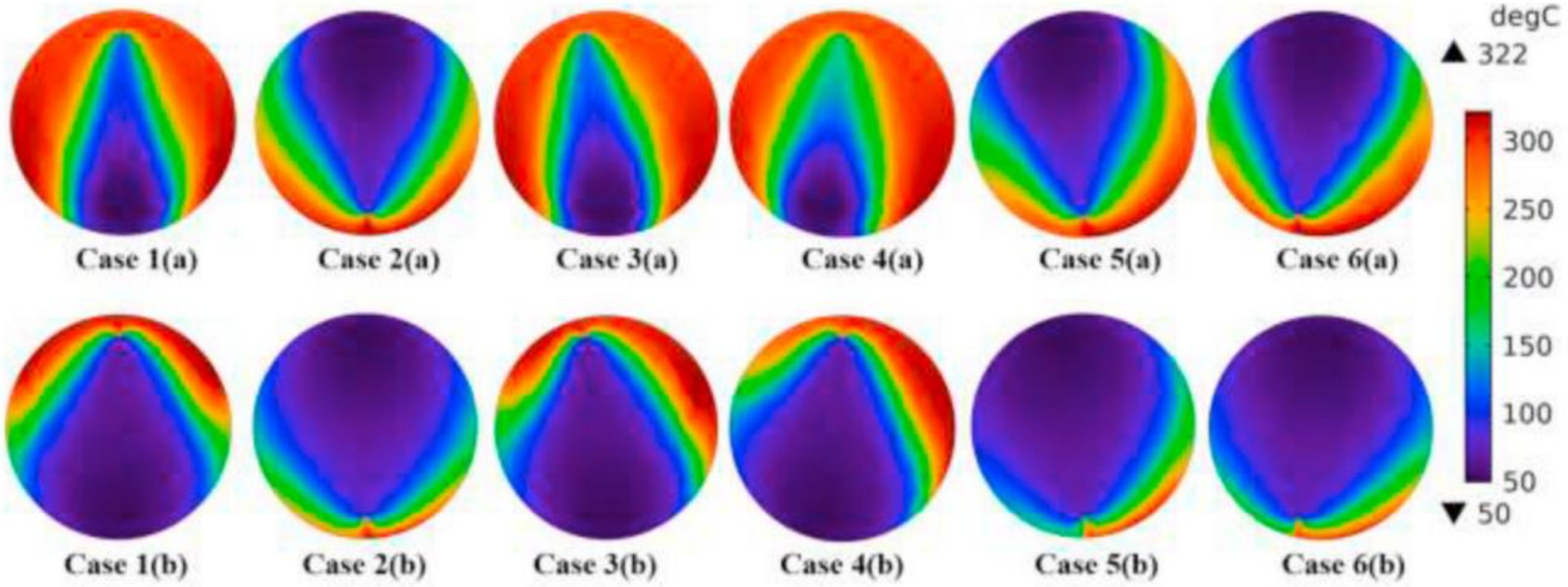

Fig. 12. Thermal front evolution for the different cases simulated at 5 years (a) and 10 years (b).

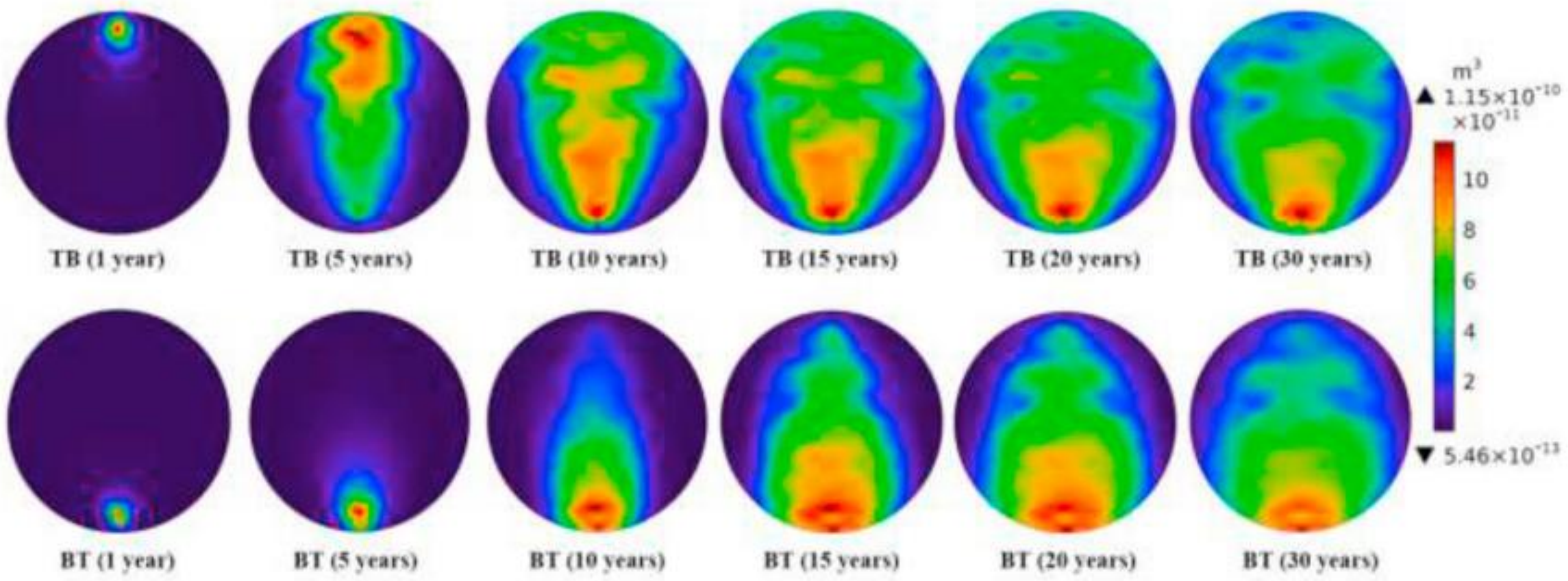

Fig. 22. Fracture transmissibility evolution on the middle fracture surface for top-bottom (TB) and bottom-top (BT) scenarios.

- Fig. 22 shows the transmissibility propagation on the fracture surfaces for the two cases. The results show that transmissibility increases during the 30 years. The increase in over time highlights that the changes emerge as the cube of the fracture aperture and not linearly with aperture. The reason for this is that the fracture is assumed to be filled with only the injected fluid, and its transmissibility to depend solely on the aperture; therefore, the flow rate increases.

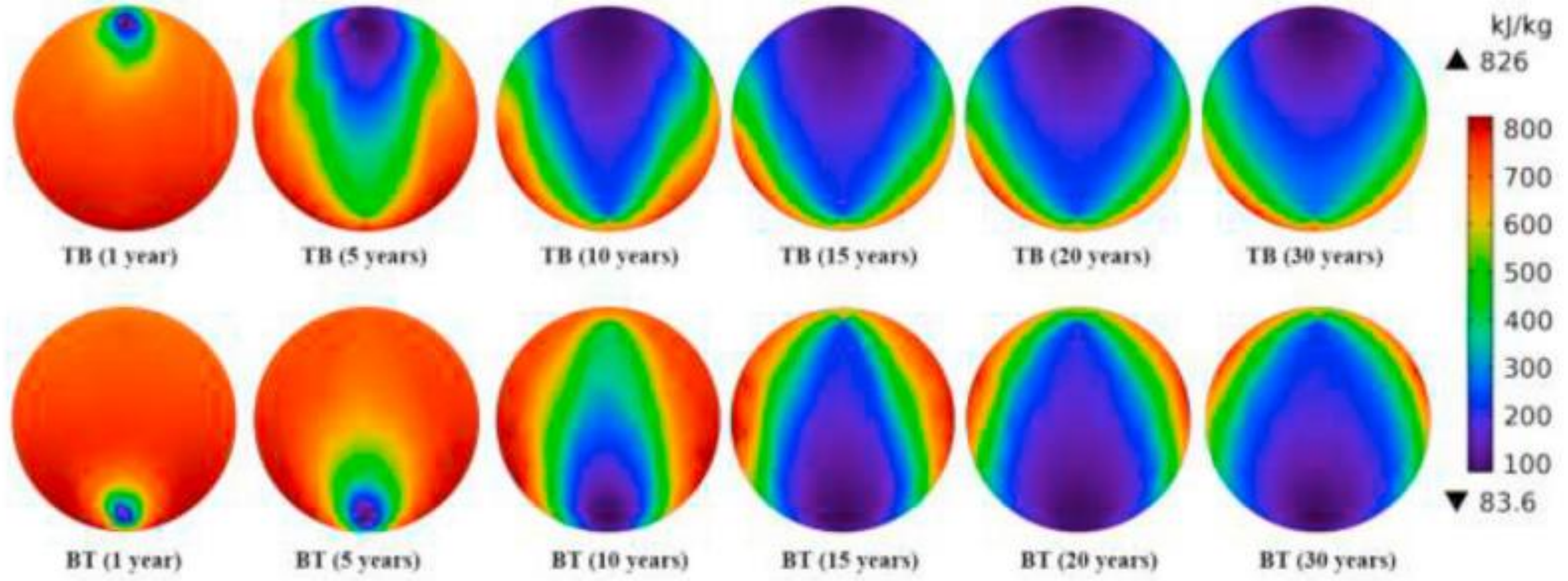

Fig. 23. Enthalpy evolution on the middle fracture surface for top-bottom (TB) and bottom-top (BT) scenarios.

- the flow path for the bottom-top scenario is obstructed by the downward force of gravity, extending the flow time and prolonging hydraulic retention. retention period in the bottom-top scenario enables the fluid to extract more energy from the rock.
- The results show that the proper configuration of wellbore design is crucial in predicting the enthalpy and lifetime of HDR geothermal reservoirs.

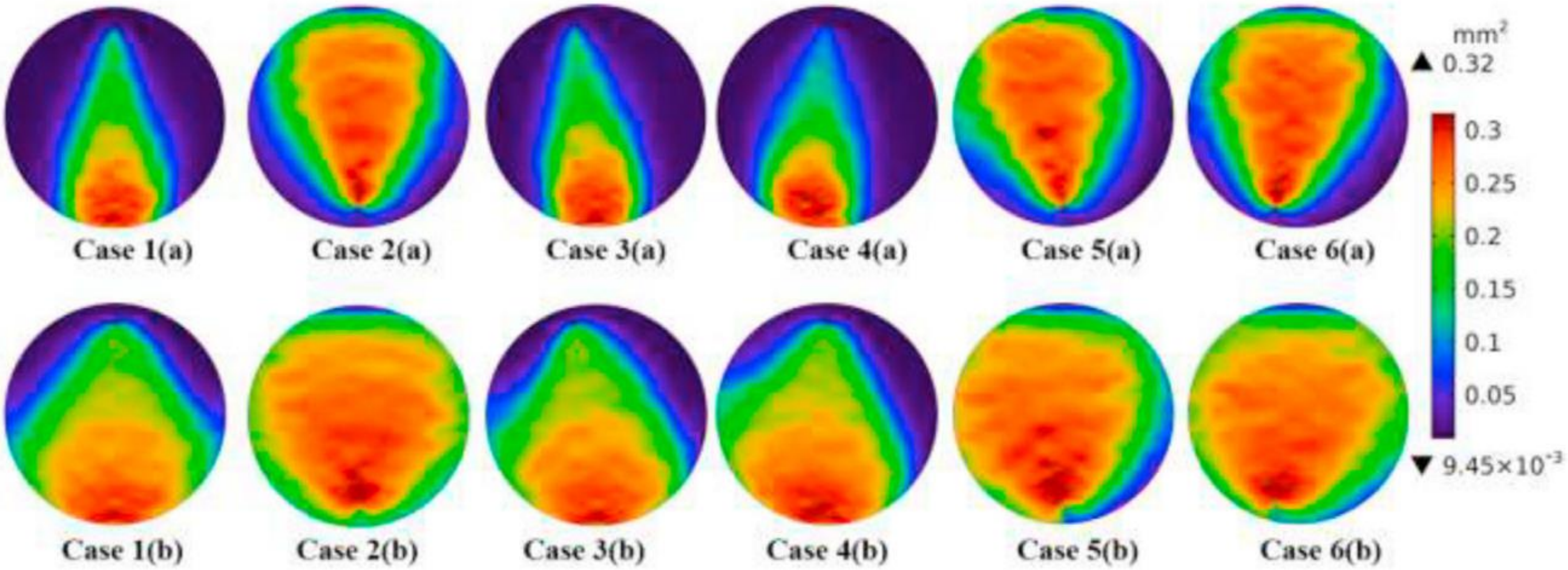

Fig. 11. Permeability changes for the different cases simulated at 5 years (a) and 10 years (b).

- The result show that the permeabilities of the fractures are more enhanced in the bottom-top scenario, leading to higher efficiency in both thermal energy and electric power generation. The increase in the fracture heat transfer area during the circulation process also increases the permeability by a relatively large magnitude. Thus, the results show that increased permeability and fracture heat transfer area result in a significant improvement in system performance.